

Bulk viscosity at high temperatures and energy densities

Abdel Nasser Tawfik*

*Nile University, Egyptian Center for Theoretical Physics (ECTP),
Juhayna Square of 26th-July-Corridor, 12588 Giza, Egypt and
Goethe University, Institute for Theoretical Physics (ITP),
Max-von-Laue-Str. 1, D-60438 Frankfurt am Main, Germany*

Carsten Greiner

*Goethe University, Institute for Theoretical Physics (ITP),
Max-von-Laue-Str. 1, D-60438 Frankfurt am Main, Germany*

(Dated: November 11, 2019)

For temperatures (T) ranging from a few MeV up to TeV and energy density (ρ) up to 10^{16} GeV/fm³, the bulk viscosity (ζ) is calculated in non-perturbation and perturbation theory with up, down, strange, charm, and bottom quark flavors, at vanishing baryon-chemical potential. The effective QCD-like model, the Polyakov linear-sigma model, comes up with essential contributions for the vacuum and thermal condensations of gluons and quarks (up, down, strange, and charm). The thermodynamic contributions of photons, neutrinos, charged leptons, electroweak particles, and the scalar Higgs boson, are found significant along the entire range of T and ρ . We conclude that the dimensionless quantity $9\omega_0\zeta/Ts$, where ω_0 is a perturbative scale and s is the entropy density, decreases exponentially with increasing T , while the increase ρ is accompanied with an almost linear increase in ζ up to 10^{14} GeV³. Certainly, these results offer a great deal to explore in cosmology, for instance.

PACS numbers: 67.57.Hi, 12.38.Gc, 31.15.Md

Keywords: Transport properties, Lattice QCD calculations, Perturbation theory

Contents

I. Introduction	2
II. Theoretical approach	3
A. Formula for bulk viscosity	3
1. Boltzmann-Uehling-Uhlenbeck (BUU) Approach	3
2. Green-Kubo (GK) Approach	5
B. Quark condensates	7
1. Vacuum quark condensates	7
2. Quark condensates at finite temperature	8
C. Gluon condensates	9
1. Vacuum gluon condensates	9
2. Gluon condensate at finite temperature	9
D. Quantum chromodynamics	9
1. Polyakov linear-sigma model (quark condensates)	9
2. Lattice QCD simulations (thermodynamic bulk viscosity)	12
III. Results and discussion	12
A. Bulk viscosity in HRGM and PLSM	12

*Electronic address: atawfik@nu.edu.eg

B. Bulk viscosity in non-perturbative and perturbative calculations	14
1. QCD contributions	14
2. SM contributions	16
IV. Conclusions	18
Acknowledgements	18
References	18

I. INTRODUCTION

High-energy experiments at the Relativistic Heavy Ion Collider (RHIC) at BNL and the Large Hadron Collider (LHC) at CERN have collected unambiguous evidences for strongly-correlated viscous QCD matter; quark-gluon plasma (QGP) [1–3]. For perturbative gauge QCD, it was suggested that the shear viscosity normalized to entropy density is very close to the lower bound predicted by Anti-de Sitter/Conformal Field Theory (AdS/CFT) [4].

On isotropic $24^2 \times 8$ and $16^2 \times 8$ lattices, the first-principle simulations for shear and bulk viscosity [5] have been calculated from *discrete* Green function in Matsubara frequencies. The viscous coefficients are determined from the slopes of the spectral functions at the vanishing Matsubara frequency. The retarded Green function as defined by Kramers-Kronig relation and given in terms of thermodynamic quantities [6] expresses the bulk viscosity as a measure for the violation of the conformal invariance. Because QCD at the classical level is conformally invariant, the quark and gluon condensates have been assumed to contribute to the bulk viscosity as well.

The quark condensates in non-perturbative QCD-like models with as much as possible quark flavors have been estimated [7, 8]. On the other hand, various thermodynamic quantities have been calculated in most reliable non-perturbative and perturbative simulations with $2 + 1 + 1 + 1$ quark flavors at vanishing baryon density [9–12]. Taking into account the contributions by the gauge bosons: photons, W^\pm , and Z^0 , the charged leptons: neutrino, electron, muon, and tau, and the Higgs bosons: scalar Higgs particle, we introduce the temperature and energy-density dependence of the bulk viscosity. The temperatures range from a few MeV and TeV, while the energy density goes from a few hundreds MeV/fm^3 to $10^{16} \text{ GeV}/\text{fm}^3$. Such a wide range does not only cover both quantum chromodynamic (QCD) and electroweak (EW) phases, which become nowadays to a some extent accessible by high-energy experiments [13] and through recent astrophysical observations [14], but also goes beyond that and approaches domains, which are likely never accessed, so far. For examples, the additional contributions by the gauge bosons, the charged leptons, and the Higgs bosons enable the energy density to approach two-order-of-magnitude GeV/fm^3 larger than the energy density reached in perturbation theory [10].

For an explanation for the simultaneous radial flow and azimuthal anisotropy in high-energy collisions [15], finite bulk viscosity was suggested as a possible mechanism [3]. Also, the interferometry correlations, i.e. the shapes of the freeze-out hyper-surface or the outer layers of the fireball and the related reduction of the ratio of two interferometry radii, can only be explained by temperature-depending bulk viscosity [16]. This is a list of a few examples on the roles that the bulk viscosity would play in hadron [3, 16–19] and QGP phases [5, 6].

The bulk viscosity as calculated during the GUT phase transition was suggested to contribute to the cosmological inflation and density fluctuations [20]. The conditions under which bulk viscosity becomes an inflationary source have been evaluated as well. It was assumed that the finite bulk viscosity considerably contributes to resolving the entropy generation problem [20, 21]. The evolution of the early Universe as described by a spatially homogeneous and isotropic Robertson-Walker model strongly depends on whether or not the viscous coefficients (bulk and/or shear) are taken finite [22–25].

The present script is organized as follows. The approaches for the bulk viscosity are introduced in section II. The Boltzmann-Uehling-Uhlenbeck (BUU) and the Green-Kubo (GK) Approachs are reviewed in section II A 1 and II A 2, respectively. The quark and the gluon condensates shall be outlined in section II B and II C, respectively. The first-principle approach, the quantum chromodynamics, is discussed in section II D, where the QCD-like approach, the Polyakov linear-sigma model (PLSM) is presented in section II D 1 and the lattice QCD simulations are given in section II D 2. The results and discussion shall be elaborated in section III. We first

start with the bulk viscosity in PLSM, section III A, and then elaborate the bulk viscosity in non-perturbative and perturbative calculations, section III B. The latter is divided into QCD contributions, section III B 1, and the Standard Model (SM) contributions, III B 2. Section IV is devoted to the final conclusions.

II. THEORETICAL APPROACH

For a system characterized by quark degrees of freedom, the equilibrium energy-momentum tensor can be given as [26]

$$T^{\mu\nu} = -p g^{\mu\nu} + \mathcal{H} u^\mu u^\nu + \Delta T^{\mu\nu}, \quad (1)$$

where $u^{\nu|\mu}$ are four velocities and p stands the pressure. The enthalpy density $\mathcal{H} = p + \rho$ is to be expressed in the energy density $\rho = -p + Ts$ and the entropy s . When inserting a dissipative part into Eq. (1), this is then derived towards out-of-equilibrium

$$\Delta T^{\mu\nu} = \eta \left(D^\mu u^\nu + D^\nu u^\mu + \frac{2}{3} \Delta^{\mu\nu} \partial_\sigma u^\sigma \right) - \zeta \Delta^{\mu\nu} \partial_\sigma u^\sigma. \quad (2)$$

In this expression, the Landau-Lifshitz condition is fulfilled, $u_\mu \Delta T^{\mu\nu} = 0$ [26] and in local rest-frame, the hydrodynamic expansion reads [26]

$$\delta T^{ij} = \sum_f \int d\Gamma^* \frac{p^i p^j}{E_f} \left[-\mathcal{A}_f \partial_\sigma u^\sigma - \mathcal{B}_f p_f^\nu D_\nu \left(\frac{\mu}{T} \right) + \mathcal{C}_f p_f^\mu p_f^\nu \left(D^\mu u^\nu + D^\nu u^\mu + \frac{2}{3} \Delta^{\mu\nu} \partial_\sigma u^\sigma \right) \right] f_f^{eq}. \quad (3)$$

The sum runs over the degrees of freedom, such as quarks and antiquarks. \mathcal{A}_f , \mathcal{B}_f and \mathcal{C}_f are functions depending on the momentum p . $d\Gamma^*$ represents a generic phase-space. It is obvious that in the local rest-frame, the given derivative vanishes, i.e. $\partial_k u_0 = 0$. This means that the sum over μ and ν is equivalent to the sum over the spatial indices ρ and σ . This leads to $p_f^i p_f^j p_f^\sigma p_f^\rho = |p_f|^4 (\delta_{ij} \delta_{\sigma\rho} + \delta_{i\sigma} \delta_{j\rho} + \delta_{i\rho} \delta_{j\sigma})$. Also, in the local rest-frame, $p_f = p$. When assuming that both Eqs. (2) and Eq. (1) are equal, then the dissipation parts of the energy-momentum tensor can be determined, straightforwardly. For all these reasons, it seems of a great advantageous to assume a local rest-frame of the fluid of interest.

The transport properties are defined as the coefficients of the spatial components of the difference between the equilibrium and out-of-equilibrium energy-momentum tensors with respect to the Lagrangian density [18]. In section II A, we discuss well-known approaches for the viscous coefficients, namely the Boltzmann-Uehling-Uhlenbeck (BUU), section II A 1 and Green-Kubo (GB) approach, section II A 2.

A. Formula for bulk viscosity

1. Boltzmann-Uehling-Uhlenbeck (BUU) Approach

For an equilibrium state having f quark flavors with momenta \vec{p} , the phase-space distribution for these fermions including the Polyakov loop variables can be expressed as [27]

$$f_f(T, \mu) = \ln \left[1 + 3 \left(\phi + \phi^* e^{-\frac{E_f - \mu_f}{T}} \right) \times e^{-\frac{E_f - \mu_f}{T}} + e^{-3 \frac{E_f - \mu_f}{T}} \right]. \quad (4)$$

where $E_f = (m_f^2 + p^2)^{1/2}$ is the dispersion relation of f -th quark flavor. A similar expression can be deduced for anti-quarks, where ϕ and ϕ^* are exchanged and $-\mu_f \rightarrow +\mu_f$. We also express Eq. (4) in terms of ϕ and ϕ^* , the Polyakov loop variables, Eq. (61). This expression shall be needed when utilizing PLSM, section II D 1, in determining the bulk viscosity and also for the temperature dependence of the different quark condensates, section II B.

At finite temperature and density, the relaxation time approximation, for example, can be applied to the Boltzmann-Uehling-Uhlenbeck (BUU) expression [19] with Chapman-Enskog expansion. In non-Abelian external field, the viscous coefficients can be estimated from relativistic kinetic theory. As we focus on the Bulk viscosity, this is given as [19],

$$\zeta(T, \mu) = \frac{1}{9T} \sum_f \int \frac{d^3p}{(2\pi)^3} \frac{\tau_f}{E_f^2} \left[\frac{|\vec{p}|^2}{3} - c_s^2 E_f^2 \right]^2 f_f(T, \mu). \quad (5)$$

For macroscopic consideration, the relaxation time τ_f , which involves complicated collision integrals, could be for simplicity determined as the mean collision time and thus from thermal averages [23, 24, 28]

$$\tau_f(T) = \frac{1}{n_f(T) \langle v(T) \rangle \sigma(T)}, \quad (6)$$

where $\langle v(T) \rangle$ is the mean relative velocity of two colliding particles, σ is the cross section, and $n_f(T)$ is the corresponding number density. Approaches to determine $\langle v(T) \rangle$ and σ have been discussed in ref. [24], for instance.

When adding a small perturbation, i.e. even the local equilibrium is slightly derived towards an out-of-equilibrium status, the four velocity $u^\mu(x)$ become no longer constant in space and time, then the energy-momentum tensor $T^{\mu\nu}$ and the distribution function $f_f(T, \mu)$, for instance, depart from the thermal equilibrium, as well,

$$\delta T^{jj} = \sum_f \int \frac{d^3p}{(2\pi)^3} \frac{p^i p^j}{E_f} f_f^{eq}(u_i p^i / T) \phi_f(x, p), \quad (7)$$

$$f_f(x, p) = f^{eq}(u_i p^i / T) \left[1 + \phi_f(x, p) \right], \quad (8)$$

$$\phi_f = \left[-\mathcal{A}_f \partial_\sigma u^\sigma - \mathcal{B}_f p_f^\nu D_\nu \left(\frac{\mu}{T} \right) + \mathcal{C}_f p_f^\mu p_f^\nu \left(D^\mu u^\nu + D^\nu u^\mu + \frac{2}{3} \Delta^{\mu\nu} \partial_\sigma u^\sigma \right) \right]. \quad (9)$$

In order to determine \mathcal{A}_f and \mathcal{C}_f , we recall the Boltzmann master equation [19], which can be expressed as

$$\frac{\partial f_f(x, t, p)}{\partial t} = \left(\frac{\partial}{\partial t} + \frac{\partial}{\partial x^i} \frac{\partial x^i}{\partial t} + \frac{\partial}{\partial p^i} \frac{\partial p^i}{\partial t} \right) f_f(x, t, p). \quad (10)$$

The right-hand side gives the collision integral. For a collision such as $\{i\} \leftrightarrow \{j\}$, the equilibrium distribution functions are identical, $f_{\{i\}}^{eq} = f_{\{j\}}^{eq}$ [19] and the collision integral can be given as

$$\mathbf{C}[f_f] = \sum_{\{i\}\{j\};f} \frac{1}{S} \int \left(\frac{dk_z}{2\pi} \right)_{\{i\}} \left(\frac{dk_z}{2\pi} \right)_{\{j\}} W(\{i\}|\{j\}) F[f_f], \quad (11)$$

in which the statistical factor S takes into consideration identical particles. $F[f_f]$ expresses Bose-Einstein or Fermi-Dirac distribution statistics [19],

$$F[f_f] = \Pi_{\{i\}} \Pi_{\{j\}} \{ f_j (1 + (-1)^{s_i} f_i) - f_i (1 + (-1)^{s_j} f_j) \}. \quad (12)$$

Due to Landau-Lifshitz condition, some constrains can be added to $\phi_f(x, p)$, Eq. (9), so that $|\phi_f| \ll 1$ [19]. Under these assumptions, a particular solution that conserves Landau-Lifshitz condition, as well, can be proposed as [19, 27].

$$\mathcal{A}_f = \mathcal{A}_f^{\text{par}} - b E_f, \quad (13)$$

$$\mathcal{A}_f^{\text{par}} = \frac{\tau_f}{3T} \left[\frac{|\vec{p}|^2}{3} - c_s^2 E_f^2 \right], \quad (14)$$

where τ_f is the relaxation time, Eq. (6), which can be for instance linked to the decay width as discussed in refs. [28, 29], and $c_s^2 = \partial p / \partial \rho$ is the speed of sound squared.

In relaxation time approximation [27], the phase-space distributions of quarks and antiquarks can be replaced by their equilibrium ones; $f = f^{eq} + \delta f$, where δf is allowed to be arbitrary infinitesimal, while the collision integral can be approximated as $\mathbf{C}[f_f] = \delta f / \tau_f$ [19]. Then, the particular solution $\mathcal{A}_f^{\text{par}}$, Eq. (14), is also valid. Furthermore, we get [19],

$$\mathcal{C}_f^{\text{par}} = \frac{\tau_f}{2TE_f}. \quad (15)$$

2. Green-Kubo (GK) Approach

In Lehmann spectral representation of two-point correlation functions of the energy-momentum tensor, the Green-Kubo formalisms for bulk and shear viscosity can be expressed as [30, 31]

$$\begin{pmatrix} \zeta \\ \eta \end{pmatrix} = \lim_{\omega \rightarrow 0^+} \lim_{|\mathbf{p}| \rightarrow 0^+} \frac{1}{\omega} \begin{pmatrix} \frac{1}{2} A_\zeta(\omega, |\mathbf{p}|) \\ \frac{1}{20} A_\eta(\omega, |\mathbf{p}|) \end{pmatrix}, \quad (16)$$

where A_ζ and A_η are spectral functions [30]

$$A_\zeta(\omega, |\mathbf{p}|) = \int d^4x e^{ip \cdot x} \langle [\mathcal{P}(x), \mathcal{P}(0)] \rangle, \quad (17)$$

$$A_\eta(\omega, |\mathbf{p}|) = \int d^4x e^{ip \cdot x} \langle [\pi^{ij}(x), \pi^{ij}(0)] \rangle, \quad (18)$$

$$\mathcal{P}(x) = -\frac{1}{3} T_i^i(x) - c_s^2 T^{00}(x), \quad (19)$$

$$\pi^{ij}(x) = T^{ij}(x) - \frac{1}{3} \delta^{ij} T_k^k(x), \quad (20)$$

and $\langle [\dots] \rangle$ stands for an appropriate thermal averaging.

For simplicity, we limit the discussion to shear viscosity, which is similar to the bulk viscosity. When expressing the energy-momentum tensor in terms of the Lagrangian density [27], we get

$$T^{\mu\nu} = -g^{\mu\nu} \mathcal{L} + \frac{\partial \mathcal{L}}{\partial(\partial_\mu \Phi)} \partial^\nu \Phi. \quad (21)$$

The viscous stress tensor is then determined by the Lagrangian part, for instance,

$$\pi_{\mu\nu} = \left(\Delta_{\mu\nu} \Delta^{\rho\sigma} - \frac{1}{3} \Delta_{\mu\rho} \Delta^{\nu\sigma} \right) T^{\rho\sigma}, \quad (22)$$

where $\Delta^{\mu\nu} = g^{\mu\nu} - u^\mu u^\nu$.

In linear response theory (LRT), we can estimate the impacts of the dissipative forces on the energy-momentum tensor. It is obvious to expect that these forces are small relative to the typical energies of the system of interest, especially in strongly interacting systems [32], as what we are dealing with in the present paper. The linear response of the microscopic viscous stress-tensor, for instance, $\pi^{\mu\nu}$, to the dissipative forces, makes it possible to relate the correlation functions to the macroscopic viscosity parameter [33]. With an appropriate thermal averaging of two-point function, $\langle \dots \rangle$, two point correlator of the viscous stress-tensor can be deduced as

$$\Pi_{ab}(|\mathbf{p}|) = i \int d^4x e^{ip \cdot x} \langle \tau_c \pi_{\mu\nu}(x) \pi^{\mu\nu}(0) \rangle^{ab}, \quad (23)$$

where $a, b \in [1, 2]$ represents the thermal indices of 2×2 -matrix for $\langle \dots \rangle$ and τ_c is time ordering with respect to a contour in the complex time plane.

The spectral function can be written as

$$A_\eta(\omega, |\mathbf{p}|) = 2 \tanh\left(\frac{\omega/T}{2}\right) \text{Im} \Pi_{11}(\omega, p). \quad (24)$$

The diagonal element can be related to the retarded two-point function of the viscous stress-tensor. There are 11 components [32]

$$\Pi_{11}(|\mathbf{p}|) = i \int d\Gamma^* N(p, k) D_{11}(k) D_{11}(p - k), \quad (25)$$

where $D_{11}(p)$ is the scalar part of the 11 components of the quark-propagator matrix and $N(p, k)$ includes the numerator part of the propagators. Further details are now in order. These can be summarized as follows.

- The 11 components of the scalar part of the thermal propagator can be expressed using formalism of real-time thermal field theory (RFT)

$$D^{11}(k) = \frac{-1}{k_0^2 - E_{B,f}^2 + i\rho} - 2\pi i E_{B,f}(E_k) f_f(k) \delta(k_0^2 - E_{B,f}^2(k)). \quad (26)$$

When replacing the momentum indices $p \rightarrow k$ in Eq. (4), the Fermi-Dirac distribution function and the modified dispersion relation can be expressed in terms of the Polyakov-loop variables as well.

- The remaining parts in Eq. (25) stand for fermions [31, 32, 34], where

$$N(p, k) = \frac{32}{3} k_0(k_0 + \omega) \mathbf{k} \cdot (\mathbf{k} + \mathbf{p}) - 4 \left(\mathbf{k} \cdot (\mathbf{k} + \mathbf{p}) + \frac{1}{3} \mathbf{k}^2 (\mathbf{k} + \mathbf{p})^2 \right). \quad (27)$$

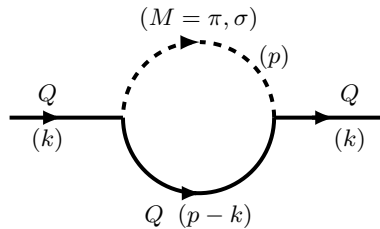


Fig. 1: A schematic one-loop diagram diagram of quark-meson loops taken from [27].

Fig. 1 depicts one-loop diagram of quark-meson loops. For PLSM, section IID 1, we limit the discussion to π and σ mesons, which can then be obtained from the two-point correlation function of the viscous stress-tensor, at vanishing frequency and momentum [32]. The dashed lines stands for the quark propagators, which have a finite thermal widths. The thermal width can be deduced from the quark self-energy diagram [35]. In PLSM, section IID 1, the shear viscosity, Eq. (16), can be rewritten as [27]

$$\eta = \lim_{\omega \rightarrow 0^+} \lim_{|\mathbf{p}| \rightarrow 0^+} \frac{\text{Im} \Pi_{11}(\omega, p)}{10\omega} = \frac{1}{10} \lim_{\omega \rightarrow 0^+} \lim_{|\mathbf{p}| \rightarrow 0^+} \text{Im} \left[\sum_f \int \frac{dk}{2\pi} \frac{(-N)}{E_f(k)E_f(p+k)} \right. \\ \left. \lim_{\Gamma \rightarrow 0} \left(\frac{C^-/\omega}{[\omega - E_f(k) + E_f(p+k)] + i\Gamma} + \frac{C^+/\omega}{[\omega + E_f(k) - E_f(p+k)] + i\Gamma} \right) \right], \quad (28)$$

$$\eta(T, \mu) = \frac{2}{15T} \sum_f \int \frac{d^3p}{(2\pi)^3} \frac{|\vec{p}|^4 \tau_f}{E_f^2} f_f(T, \mu) [1 + f_f(T, \mu)], \quad (29)$$

where $C^\mp = \mp f_f(k)^\mp + f_f(p+k)^\mp [\mp\omega + E_{B,f}(k)]$.

Then, the bulk viscosity, at finite temperature, T , and chemical potential, μ , reads [27]

$$\zeta(T, \mu) = \frac{3}{2T} \sum_f \int \frac{d^3p}{(2\pi)^3} \frac{\tau_f(T, \mu)}{E_f^2} \left[\frac{|\vec{p}|^2}{3} - c_s^2 E_f^2 \right]^2 f_f(T, \mu) [1 + f_f(T, \mu)], \quad (30)$$

where $f_f(T, \mu)$ was expressed in Eq. (4) and $\tau_f(T, \mu)$ in Eq. (6).

B. Quark condensates

1. Vacuum quark condensates

The reason why we assume that the quark and gluon condensates either at vanishing or at finite temperatures considerably contribute to the bulk viscosity among other thermodynamic quantities is the QCD color confinement. Accordingly, the quark and gluon condensates are associated with the dynamics of hadron wavefunctions, but not necessarily exclusively with the vacuum [36].

In late sixtieth of the last century Gell-Mann, Oakes, and Renner have shown that the masses squared of the Nambu-Goldstone bosons are proportional to the masses of the light quarks [37],

$$m_\pi^2 = A(m_u + m_d) + \mathcal{O}(m^2), \quad A = \left| \frac{\langle 0 | \bar{\psi}\psi | 0 \rangle}{f_\pi^2} \right|_{m_u, m_d \rightarrow 0}, \quad (31)$$

where $|\langle \bar{\psi}\psi \rangle| = |(\bar{u}u + \bar{d}d)|/2 = 8\pi f_\pi^3/\sqrt{3}$ [38]. Eq. (31) was originally derived up to terms linear in the quark masses. The perturbative corrections are conjectured to contribute to improving its uncertainty; less than 10% [39]. As pointed out by Weinberg [40], the chiral symmetry determines the low-energy interactions between the Nambu-Goldstone bosons, the pions, in terms of the pion decay constant, for instance, due to the limit that the velocities of the incoming pions become low or their center-of-mass energy approaches m_π^2 . Thus, the amplitude of their elastic collision inclines to $\sim 3m_\pi^2/f_\pi^2$, and the proportionality constant A is related to the light quark condensates. Apart from the higher order corrections, Eq. (31) obviously states that the masses of the low-lying Nambu-Goldstone bosons are given by the product of the quark condensates and masses. While the quark condensates measure the strength of spontaneous symmetry breaking, the quark masses themselves are - in turn - responsible for the chiral symmetry breaking in the QCD Lagrangian. Eq. (31) can be rewritten as [41]

$$\langle 0 | \bar{q}q | 0 \rangle \simeq \frac{m_\pi^2}{m_u + m_d} f_\pi^2. \quad (32)$$

At physical decay constant $f_\pi = 130.41 \pm 0.03$ MeV [42], $|\langle \bar{q}q \rangle| = (338.144 \text{ MeV})^3$.

Assuming isospin symmetry, the pion mass can be determined from the pole position in the two-point function under Fourier transform of $\langle 0 | T A_\mu^i(x) A_\nu^k(y) | 0 \rangle$, where the operator T denotes the time ordering assuring that the field operators are to be ordered so that their time arguments increase from right to left, for instance. Taking into account the higher orders, the pion mass can be expressed as

$$m_\pi^2 = m^2 \left[1 + \frac{m^2}{32\pi^2 f_{\pi,\chi}^2} \ln \left(\frac{m}{\Lambda_3} \right)^2 + \mathcal{O}(m^4) \right], \quad (33)$$

where $f_{\pi,\chi}$ is the pion decay constant in the chiral limit, $m \equiv 2A m_{ud}$, with m_{ud} being the mean mass of the two light quarks. $\Lambda_3 = 0.63 \pm 0.06$ GeV [43, 44] is the renormalization group invariant scale. From (33), higher orders can be added to the physical decay constant

$$f_\pi = f_{\pi,\chi} \left[1 - \frac{m^2}{16\pi^2 f_{\pi,\chi}^2} \ln \left(\frac{m}{\Lambda_4} \right)^2 + \mathcal{O}(m^4) \right], \quad (34)$$

where $\Lambda_4 = 1.22 \pm 0.12$ GeV and the ratio of physical to chiral decay constant was estimated as $f_\pi/f_{\pi,\chi} = 1.0719 \pm 0.005$ [43, 44].

Similar to Eq. (31), other pseudoscalar mesons [41], such as kaons and eta particles, have masses much higher than that of the Nambu-Goldstone bosons, the pions, can be given as

$$m_K^2 = B(m_{ud} + m_s) + \mathcal{O}(m^2), \quad B = \left| \frac{\langle 0 | \bar{\psi}\psi | 0 \rangle}{f_K^2} \right|_{m_{ud}, m_s \rightarrow 0} \equiv A - \mathcal{O}(m_s), \quad (35)$$

$$m_\eta^2 = C(m_{ud} + 2m_s) + \mathcal{O}(m^2), \quad C = \left| \frac{\langle 0 | \bar{\psi}\psi | 0 \rangle}{f_\eta^2} \right|_{m_{ud}, m_s \rightarrow 0} \equiv \frac{2}{3} [A - \mathcal{O}(m_s)], \quad (36)$$

where up to the leading order $m_\eta^2 = (4m_K^2 - m_\pi^2)/3$ [45]. In full lattice QCD [46, 47], a recent determination of light and strange quark condensates from heavy-light current-current correlations suggests that [46, 47]

$$\frac{\langle 0|\bar{q}q|0\rangle}{\langle 0|\bar{s}s|0\rangle} = \frac{(283 \pm 2 \text{ MeV})^3}{(296 \pm 11 \text{ MeV})^3} = 0.956 \pm 0.028. \quad (37)$$

2. Quark condensates at finite temperature

As thermal systems, such as high-energy collisions, early Universe, etc. likely manifest the properties of strong interactions, the chiral symmetry, which as discussed can be measured by the quark condensates, contributes with essential information to the partition function, from which the bulk viscosity can - among many other thermal quantities - be derived. To this end, it is required that the possible thermal influences on the quark condensates can not be neglected, especially that of the lightest Nambu-Goldstone bosons, the pions. Calculations up to two loops in chiral perturbation theory proposed that the temperature dependence of the light quark condensate and the pion decay constant, respectively, reads [48]

$$\langle \bar{q}q \rangle(T) = \langle 0|\bar{q}q|0\rangle \left[1 + \frac{T^2}{8f_{\pi,\chi}^2} - \frac{T^4}{38f_{\pi,\chi}^4} + \mathcal{O}(T^6) \right], \quad (38)$$

$$f_\pi(T) = f_{\pi,\chi} \left[1 - \frac{T^2}{8f_{\pi,\chi}^2} + \mathcal{O}(T^4) \right]. \quad (39)$$

With this regard, we refer to Eq. (63), which expresses the condensates of up (σ_u), down (σ_d), and strange quark (σ_s) in dependence on the orthogonal basis transformation from $\bar{\sigma}_0$, $\bar{\sigma}_3$, and $\bar{\sigma}_8$, respectively, as calculated in PLSM.

The remaining quarks have masses heavier than the QCD scale, which is nearly of the order of the strange quark mass. These can not be treated as a small perturbation around the explicit symmetry limit, as down so far, when adding higher corrections. But up to the leading orders within the chiral limit and when taking into account $SU(4)_L \times SU(4)_R$ symmetries [49] only, the orthogonal basis transformation from $\bar{\sigma}_0$, $\bar{\sigma}_8$, and $\bar{\sigma}_{15}$, to σ_l , σ_s , and the charm quark flavor σ_c can be expressed as

$$\sigma_l = \frac{1}{\sqrt{2}}\bar{\sigma}_0 + \frac{1}{\sqrt{3}}\bar{\sigma}_8 + \frac{1}{\sqrt{6}}\bar{\sigma}_{15}, \quad (40)$$

$$\sigma_s = \frac{1}{2}\bar{\sigma}_0 - \sqrt{\frac{2}{3}}\bar{\sigma}_8 + \frac{1}{2\sqrt{3}}\bar{\sigma}_{15}, \quad (41)$$

$$\sigma_c = \frac{1}{2}\bar{\sigma}_0 - \frac{\sqrt{3}}{2}\bar{\sigma}_{15}. \quad (42)$$

As assumed, in the chiral limit, we have

$$\sigma_{l_0} = f_{\pi_\chi}, \quad (43)$$

$$\sigma_{s_0} = \frac{2f_{K_\chi} - f_{\pi_\chi}}{\sqrt{2}}, \quad (44)$$

$$\sigma_{c_0} = \frac{2f_{D_\chi} - f_{\pi_\chi}}{\sqrt{2}}. \quad (45)$$

For the sake of completeness, we emphasize that Eq. (57) could be rewritten as

$$\begin{aligned} U(\sigma_l, \sigma_s, \sigma_c) = & -h_l\sigma_l - h_s\sigma_s - h_c\sigma_c + \frac{m^2(\sigma_l^2 + \sigma_s^2 + \sigma_c^2)}{2} - \frac{c\sigma_l^2\sigma_s\sigma_c}{4} + \frac{\lambda_1\sigma_l^2\sigma_s^2}{2} \\ & + \frac{\lambda_1\sigma_l^2\sigma_c^2}{2} + \frac{\lambda_1\sigma_s^2\sigma_c^2}{2} + \frac{(2\lambda_1 + \lambda_2)\sigma_l^4}{8} + \frac{(\lambda_1 + \lambda_2)\sigma_s^4}{4} + \frac{(\lambda_1 + \lambda_2)\sigma_c^4}{4}. \end{aligned} \quad (46)$$

A comprehensive study for quark condensates at finite temperature in hadron resonance gas model (HRGM) was reported in ref. [41].

C. Gluon condensates

1. Vacuum gluon condensates

The gluon condensate was predicted by Shifman, Vainshtein, and Zakharov [50]. From the QCD sum rules for charmonium, an estimation for the renormalization invariant quantity at the lowest dimension was found finite, i.e. similar to $\langle 0|\bar{q}q|0\rangle \neq 0$,

$$\left\langle 0 \left| \frac{\alpha_s}{\pi} G_{\mu\nu} G^{\mu\nu} \right| 0 \right\rangle = 0.012 \text{ GeV}^4, \quad (47)$$

where $G^{\mu\nu}$ is the gluon field strength tensor indicating that the vacuum energy could be determined as [50]

$$\rho_0 = -\frac{9}{32} \left\langle 0 \left| \frac{\alpha_s}{\pi} G^2 \right| 0 \right\rangle, \quad (48)$$

where α_s is the running coupling constant [51]. By analyzing the vacuum-vacuum current correlators as constrained by the charmonium production, for instance, $G_{\mu\nu}G^{\mu\nu}$ can be determined even empirically, especially when recalling Meissner effect and/or the gluon contributions to the higher Fock state light-front wavefunctions of hadrons [36]

$$G_{\mu\nu}G^{\mu\nu} = 2 \sum_i (|\mathbf{B}^i|^2 - |\mathbf{E}^i|^2), \quad (49)$$

where \mathbf{B} and \mathbf{E} are magnetic and electric fields, respectively.

2. Gluon condensate at finite temperature

The relationship between the finite-temperature gluon condensates [52–56] and the trace of the energy-momentum tensor [57] and therefrom the connection with the bulk viscosity suggests that

$$G^2(T) = G_0^2 \left[1 - \left(\frac{T}{T_x} \right)^4 \right], \quad (50)$$

$$G^2(T) = G_0^2 - [\rho(T) - 3p(T)], \quad (51)$$

where

$$G^2 = -\frac{\beta(g)}{2g^3} G_{\mu\nu}G^{\mu\nu}. \quad (52)$$

The renormalization group beta function and the running coupling constant at finite temperature are given as

$$\beta(g) \simeq -\frac{1}{48\pi^2} (11 N_c - 2 n_f) g^3 + \mathcal{O}(g^5), \quad (53)$$

$$\alpha_s(T) \simeq \frac{12\pi}{(11 N_c - 2 n_f) \ln \left(\frac{T}{\Lambda_{\text{QCD}}} \right)^2}, \quad (54)$$

where Λ_{QCD} is the QCD scale and N_c and n_f are the color and quark degrees of freedom, respectively.

D. Quantum chromodynamics

1. Polyakov linear-sigma model (quark condensates)

According to BUU, section II A 1, and GK approach, section II A 2, the bulk viscosity, at least the thermal part, Eq. (5), is defined as a thermodynamic quantity. This might be related to the forcing causing or being

generated from the expansion. This would mean that as the system expands or is compressed, its thermodynamic equilibrium is perturbed, on one hand. On the other hand, the bulk viscosity belongs to the processes trying to restore equilibrium. Apparently, these are irreversible. In this section, we discuss on how to deduce QCD thermodynamic quantities from the PLSM.

Postulated for pion-nucleon interactions and chiral degrees of freedom, the linear-sigma model (LSM) [58] with a spinless scalar field σ_a [59] and the triplet pseudoscalar fields π_a is conjectured to be based on theory of quantized fields which have been introduced by Schwinger in the fifties of the last century [60–65]. This effective model has real classical field having O(4) vectors, $\vec{\Phi} = T_a(\vec{\sigma}_a, i\vec{\pi}_a)$ and $T_a = \lambda_a/2$ generators with Gell-Mann matrices λ_a . As a QCD-like approach, the chiral symmetry in LSM is conjectured to be broken explicitly by 3×3 matrix field $H = T_a h_a$, where h_a are the external fields. Also, under $SU(2)_L \times SU(2)_R$ chiral transformation $\Phi \rightarrow L^\dagger \Phi R$, the spinless scalar fields σ_a are finite. Their vacuum expectation values in turn break $SU(2)_L \times SU(2)_R$ down to $SU(2)_{L+R}$. As a result of the spontaneous symmetry breaking, the finite mean values of Φ fields, $\langle \Phi \rangle$, and of their conjugates, $\langle \Phi^\dagger \rangle$ are generated with the quantum numbers of the vacuum with $U(1)_A$ anomaly [66]. This leads to exact vanishing mean value of $\vec{\pi}_a$, the Nambu-Goldstone bosons, the pions, but assures finite mean value of $\vec{\sigma}_a$ corresponding to the diagonal generators $U(3)$ as $\vec{\sigma}_0 \neq \vec{\sigma}_3 \neq \vec{\sigma}_8 \neq 0$. Also, the quarks are expected to gain masses, where $m_q = g f_\pi$, g is the coupling and f_π is the pion decay constant. It has been shown that σ_a fields under chiral transformations exhibit a temperature behavior similar to that of the quark condensates, section II B. Thus, σ_a can be taken as order parameters for chiral phase transition [7, 67–70] and accordingly for the QCD phase structure [8, 69, 71, 72]. Various thermodynamic quantities can be estimated at finite density [27, 28, 71, 73], finite magnetic fields [27, 72, 74, 75] and finite isospin asymmetry [76].

The grand canonical partition function, \mathcal{Z} , sums the energies exchanged between particles and antiparticles, at finite temperatures, T , and/or densities, μ_f ,

$$\mathcal{Z} = \text{Tr} \exp[-(\hat{\mathcal{H}} - \sum_{f=u,d,s} \mu_f \hat{\mathcal{N}}_f)/T] = \int \prod_a \mathcal{D}\sigma_a \mathcal{D}\pi_a \int \mathcal{D}\psi \mathcal{D}\bar{\psi} \exp \left[\int_x (\mathcal{L} + \sum_f \mu_f \bar{\psi}_f \gamma^0 \psi_f) \right], \quad (55)$$

where the subscripts $f = [l, s, c, \dots]$ refer to the quark flavors, μ_f is thus the corresponding chemical potential, V is the volume of the system of interest, and $\int_x \equiv i \int_0^{1/T} dt \int_V d^3x$. It is conjectured that μ_f combines various types of chemical potentials. \mathcal{L} is summed over the chiral LSM [69, 77, 78] and Polyakov Lagrangian [79–82], $\mathcal{L} = \mathcal{L}_\chi - \mathcal{U}(\phi, \phi^*, T)$. The free energy, which can be derived as $\mathcal{F} = -T \cdot \log[\mathcal{Z}]/V$, plays a central role in thermodynamics.

$$\mathcal{F} = U(\sigma_l, \sigma_s) + \mathcal{U}(\phi, \phi^*, T) + \Omega_{\bar{q}q}(T, \mu_f, B), \quad (56)$$

where, if we limit the discussion on light and strange quarks,

- The purely mesonic potential part is given as

$$U(\sigma_l, \sigma_s) = -h_l \sigma_l - h_s \sigma_s + \frac{m^2}{2} (\sigma_l^2 + \sigma_s^2) - \frac{c}{2\sqrt{2}} \sigma_l^2 \sigma_s + \frac{\lambda_1}{2} \sigma_l^2 \sigma_s^2 + \frac{(2\lambda_1 + \lambda_2)}{8} \sigma_l^4 + \frac{(\lambda_1 + \lambda_2)}{4} \sigma_s^4, \quad (57)$$

with σ_l and σ_s represent the finite-temperature and -density versions of the light and strange quark condensates, section II B, as deduced from LSM. As discussed, the sigma fields show temperature- and density-dependence similar to that of the quarks and therefore play the role as order parameters.

- The Polyakov loop potentials [79–82], introduce gluonic degrees-of-freedom and dynamics of the quark-gluon interactions to the chiral LSM. The polynomial logarithmic parametrisation potential can be given as [83]

$$\begin{aligned} \frac{\mathcal{U}_{\text{PolyLog}}(\phi, \phi^*, T)}{T^4} &= \frac{-a(T)}{2} \phi^* \phi + b(T) \ln [1 - 6 \phi^* \phi + 4(\phi^{*3} + \phi^3) - 3(\phi^* \phi)^2] \\ &+ \frac{c(T)}{2} (\phi^{*3} + \phi^3) + d(T) (\phi^* \phi)^2. \end{aligned} \quad (58)$$

where $x(T) = [x_0 + x_1 (T0/T) + x_2 (T0/T)^2] / [1 + x_3 (T0/T) + x_4 (T0/T)^2]$ and $b(T) = b_0 (T0/T)^{b_1} [1 - e^{b_2 (T0/T)^{b_3}}]$, with $x = (a, c, d)$. These coefficients a , c , and d have been determined in ref. [83],

- The quarks and antiquark potentials, at finite T and μ_f [84], read

$$\Omega_{\bar{q}q}(T, \mu_f) = -2T \sum_f \int_0^\infty \frac{d^3\vec{p}}{(2\pi)^3} f_f(T, \mu) \left\{ \ln \left[1 + 3 \left(\phi + \phi^* e^{-\frac{E_f - \mu_f}{T}} \right) e^{-\frac{E_f - \mu_f}{T}} + e^{-3\frac{E_f - \mu_f}{T}} \right] \right. \\ \left. + \ln \left[1 + 3 \left(\phi^* + \phi e^{-\frac{E_f + \mu_f}{T}} \right) e^{-\frac{E_f + \mu_f}{T}} + e^{-3\frac{E_f + \mu_f}{T}} \right] \right\}, \quad (59)$$

When introducing Polyakov-loop corrections to the quark's degrees of freedom, then the corresponding Fermi-Dirac distribution function is the one given in Eq. (4).

By using thermal expectation value of a color traced Wilson loop in the temporal direction [85],

$$\Phi(\vec{x}) = \frac{1}{N_c} \langle \mathcal{P}(\vec{x}) \rangle, \quad (60)$$

then, the Polyakov-loop potential and that of its conjugate manifest QCD dynamics can be given as

$$\phi = (\text{Tr}_c \mathcal{P})/N_c, \quad \phi^* = (\text{Tr}_c \mathcal{P}^\dagger)/N_c, \quad (61)$$

where \mathcal{P} is the Polyakov loop, which can be represented by a matrix in color space [85]

$$\mathcal{P}(\vec{x}) = \mathcal{P} \exp \left[i \int_0^\beta d\tau A_4(\vec{x}, \tau) \right], \quad (62)$$

where $\beta = 1/T$ stands for the inverse temperature and $A_4 = iA^0$ is the Polyakov gauge [85, 86].

For sake of a greater elaboration, we recall that the Polyakov loop matrix can be represented as a diagonal representation [87]. The Polyakov loop and the quarks are coupled. This is given by the covariant derivative $D_\mu = \partial_\mu - iA_\mu$, in which $A_\mu = \delta_{\mu 0} A_0$ is restricted to the chiral limit. As discussed, the PLSM Lagrangian is invariant under chiral flavor group, similar to the QCD Lagrangian [79, 81, 82].

In pure gauge limit, no quark flavors, we find that $\phi = \phi^*$ and each of them is taken as an order parameter for the QCD deconfinement phase transition [79, 80]. In order to take into account the thermodynamic behavior, we use a temperature-dependent potential $U(\phi, \phi^*, T)$, Eq. (58). When comparing the PLSM results with the lattice QCD simulations, $Z(3)$ center symmetry is found similar to that of the pure gauge QCD Lagrangian [79, 80].

As discussed, the mean values of $\langle \Phi \rangle$ and that of $\langle \Phi^\dagger \rangle$ are generated with the quantum numbers of the vacuum with $U(1)_A$ anomaly. Also, $\bar{\sigma}_3$ breaks the isospin symmetry $SU(2)$ [66] and h_a , where $H = T_a h_a$. Accordingly, the diagonal components of the symmetry generators h_0, h_3, h_8 are finite leading to three finite condensates $\bar{\sigma}_0, \bar{\sigma}_3$ and $\bar{\sigma}_8$ and $m_u \neq m_d \neq m_s$. It would be convenient to convert the condensates by the orthogonal basis transformation from the original basis, $\bar{\sigma}_0, \bar{\sigma}_3$, and $\bar{\sigma}_8$ to pure up (σ_u), down (σ_d), and strange (σ_s) quark flavor basis, respectively,

$$\begin{bmatrix} \sigma_u \\ \sigma_d \\ \sigma_s \end{bmatrix} = \frac{1}{\sqrt{3}} \begin{bmatrix} \sqrt{2} & 1 & 1 \\ \sqrt{2} & -1 & 1 \\ 1 & 0 & -\sqrt{2} \end{bmatrix} \begin{bmatrix} \bar{\sigma}_0 \\ \bar{\sigma}_3 \\ \bar{\sigma}_8 \end{bmatrix}. \quad (63)$$

Thus, the masses of u, d , and s quarks can be given as,

$$m_u = \frac{g}{2} \bar{\sigma}_u, \quad (64)$$

$$m_d = \frac{g}{2} \bar{\sigma}_d, \quad (65)$$

$$m_s = \frac{g}{\sqrt{2}} \bar{\sigma}_s. \quad (66)$$

When assuming global minimization of the free energy (\mathcal{F}),

$$\left. \frac{\partial \mathcal{F}}{\partial \sigma_l} = \frac{\partial \mathcal{F}}{\partial \sigma_s} = \frac{\partial \mathcal{F}}{\partial \phi} = \frac{\partial \mathcal{F}}{\partial \phi^*} \right|_{min} = 0, \quad (67)$$

the remaining parameters $\sigma_l = \bar{\sigma}_l$, $\sigma_s = \bar{\sigma}_s$, $\phi = \bar{\phi}$ and $\phi^* = \bar{\phi}^*$ and their dependence on T and μ can be determined. Having the thermodynamic free energy constructed, Eq. (55), and assuring global minimization, Eq. (67), the different thermodynamic quantities can be estimated. Substituting the thermodynamic quantities in Eq. (5), the bulk viscosity can be evaluated at finite T and μ .

2. Lattice QCD simulations (thermodynamic bulk viscosity)

Pioneering lattice QCD simulations for viscosity has been reported in ref. [5]. This was possible through accumulating a large amount of configurations for *discrete* Green function, Eqs. (17) and (18) in Matsubara frequencies on isotropic $24^2 \times 8$ and $16^2 \times 8$ lattices. The viscous coefficients are determined as slopes of the spectral functions at vanishing Matsubara frequency. The lattice results on ζ/s are depicted in top panel of Fig. 3.

Another milestone was set by ref. [6, 88], in which Eq. (24) and its relation to the retarded Green function as defined by the Kramers-Kronig relation and given in Eq. (28) are expressed in terms of thermodynamic quantities. Furthermore, the authors of ref. [6] took into consideration the fact that the bulk viscosity also measures the violation of the conformal invariance. Thus, it was pointed out that the QCD at the classical level is conformally invariant. This was the reason why quark and gluon condensates, sections IIB and IIC, have also been proposed to contribute to the bulk viscosity,

$$\begin{aligned} \zeta = & \frac{1}{9\omega_0} \left[T s \left(\frac{\partial \rho}{\partial p} - 3 \right) - 4(\rho - 3p) \right. && \text{thermal parts} \\ & + \left(T \frac{\partial}{\partial T} - 2 \right) \langle \bar{q}q \rangle(T) + g_g G^2(T) && \text{thermal q \& g condensates} \\ & \left. + g_f (m_\pi^2 f_\pi^2 + m_K^2 f_K^2 + m_D^2 f_D^2 + \dots) \right]. && \text{vacuum q \& g condensates} \end{aligned} \quad (68)$$

where g_g and g_f are the degeneracy factors for gluon and quarks, respectively. $g_g = 16$ (spin polarization multiplied by $N_c^2 - 1$) and N_c is the color degrees of freedom. $g_f = 12 n_f$ (spin polarization multiplied by parity multiplied by $N_c \times n_f$, where n_f are the degrees of freedom of the quark flavors. m_D and f_D stand for mass and decay constant of D -meson, respectively.

The scale parameter ω_0 defines the applicability of perturbation theory. In Eq. (68), ζ was obtained using the frequency limit of the spectral density at vanishing spatial momentum [6, 89].

At $T > T_c$, a combination of low-energy theorems, as detailed in sections IIB and IIC and in the second line of Eq. (68) with finite-temperature non-perturbative calculations, first line of Eq. (68) was studied in ref. [88] and later on introduced in ref. [6]. At $T < T_c$, the same approach was utilized to obtain the upper bounds on the shear and bulk viscosity normalized to the entropy density.

III. RESULTS AND DISCUSSION

A. Bulk viscosity in HRGM and PLSM

To draw a picture for the temperature dependence of ζ around the quark-hadron phase transition, we confront our PLSM calculations with recent lattice QCD results [5] and compare these with the HRGM estimations. From the convincing agreement above T_c , the integrability with the HRGM calculations, and the resulting parameterizations various conclusions can be drawn now. First, they affirm the certainty of the methodology utilized in the present work, namely, Eq. (68) as deduced from BUU and KG approaches. The KG approach was also utilized in the lattice QCD simulations [5], as elaborated in section IID2. Second, they propose an

essential extension to temperatures below T_c and accordingly help in characterizing the possible impacts the quark-hadron phase transition on ζ , which are apparently very significant. Last but not least, they motivate the attempt of the present work to cover a wider range of higher temperatures and then to initiate implications in heavy-ion collisions [90] and physics of early Universe [12].

It is worthy highlighting that the HRGM and PLSM calculations are based on Eq. (30), which in turn is equivalent to the first line of Eq. (68). The same was done in generating the lattice QCD calculations [5]. The results, which are based on the entire Eq. (68), shall be presented in section III B.

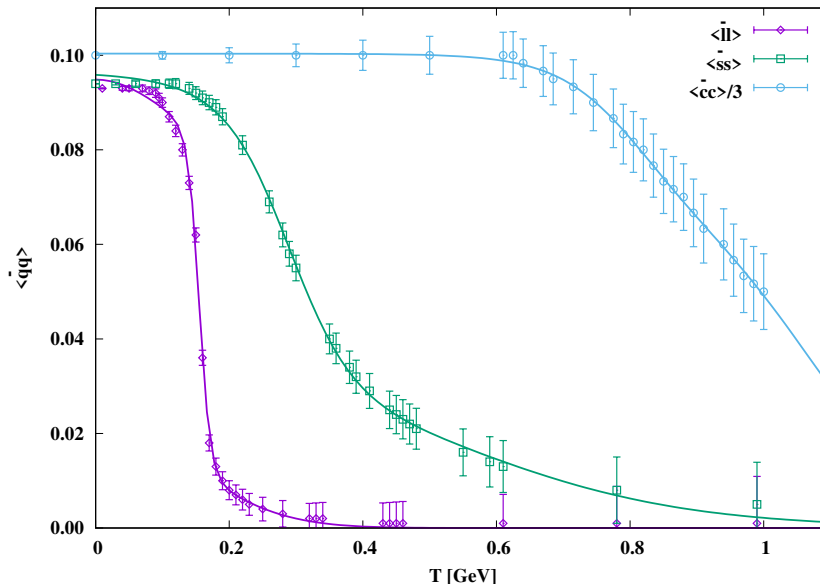


Fig. 2: (Color online) The temperature dependence of light, strange, and charm quark condensates as calculated in PLSM (symbols), at vanishing baryon-chemical potential. The curves represent binomial parameterizations.

We first start with the main contributions from PLSM, namely the quark condensates. Fig. 2 depicts the temperature dependence of light, strange, and charm quark condensates. The symbols represent the PLSM calculations, Eq. (63). The curves are binomial parameterizations. We notice that both light and strange quark condensates almost diminish at the QCD critical temperature. At high temperatures the dominant contribution to the bulk viscosity is stemming from the charm condensate. The contributions that the quarks and gluons come up with to the bulk viscosity are illustrated in left panel of Fig. 5. Accordingly, it is likely that the still missing bottom and top quark condensates, as shall be elaborated in section III B, become dominant at higher temperatures or larger energy densities. We also notice that the temperature dependence is very structured, i.e. non-monotonic.

In Fig. 3, the dimensionless ζ/s is depicted in dependence on T/T_c . The results of PLSM (squares) and HRGM (diamonds) are compared with the lattice QCD simulations (circles) [5]. Presenting results on ζ/s , which are also calculated with the same approach as the lattice QCD [5], affirms the correctness of PLSM (squares) and HRGM (diamonds).

At $T < T_c$, the HRGM results match well with PLSM and lattice QCD. Due to the huge decrease with increasing T , we draw the results in log-log scale. A similar result shall be reposted in section III B, in which recent lattice QCD simulations with $2 + 1 + 1 + 1$ quark flavors at a wide range of temperatures are taken into consideration. The lattice QCD simulations [5] are limited to temperatures $> T_c$. With the present study we cover $\leq T_c$ by HRGM (diamonds) [18], as well. At $T \leq T_c$, we notice that ζ/s rapidly decreases with the increase in T . This might be understood - among others - due to quark condensates and interaction measure, which set on their decrease and increase, respectively, with increasing temperature, especially within the region of the QCD phase transition (crossover). At $T > T_c$, the lattice QCD [5] and the PLSM calculations (squares) both indicate that ζ/s drops and keeps its small value over a wide range of temperatures. The reason would be the large entropy density (s/T^3) and the decreasing interaction measure $[(\rho - 3p)/T^4]$ above T_c .

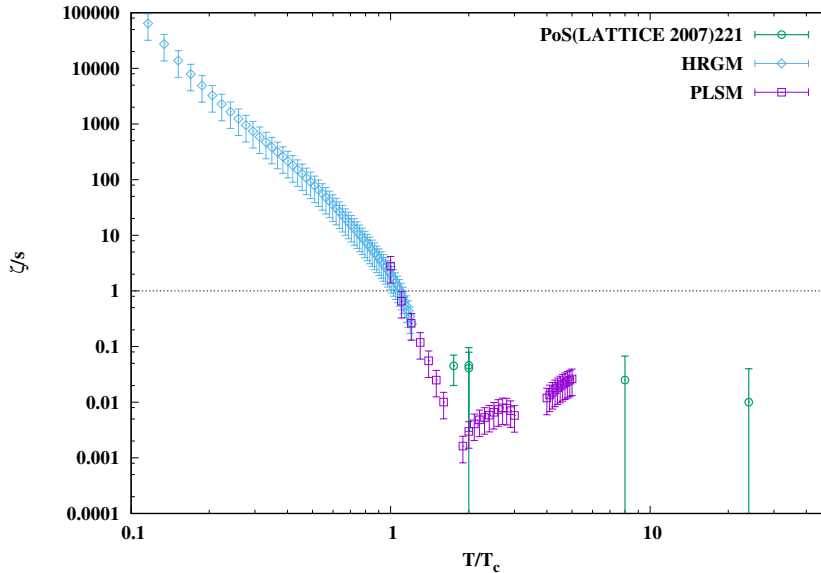


Fig. 3: (Color online) At vanishing baryon-chemical potential, the temperature dependence of ζ/s as calculated in lattice QCD (circles) and PLSM (squares) above T_c with the HRGM (diamonds) below T_c . The curves present parameterizations.

To draw a picture about the entropy density, we recall the Stefan-Boltzmann (SB) approach. The various thermodynamic quantities can be derived from the partition function characterizing an ideal gas of free quarks and gluons [91]. For example, the entropy density reads

$$\frac{s_{\text{SB}}}{T^3} = \frac{2\pi^2}{45}g_g - \frac{1}{6}\sum_f g_f \left[\left(\frac{\mu_f}{T}\right)^2 + \frac{1}{\pi^2}\left(\frac{\mu_f}{T}\right)^4 \right] + \frac{2}{45}\sum_f g_f \left[\frac{7}{4}\pi^2 + \frac{15}{2}\left(\frac{\mu_f}{T}\right)^2 + \frac{15}{4\pi^2}\left(\frac{\mu_f}{T}\right)^4 \right]. \quad (69)$$

At vanishing μ_f , $n_f = 3$, $g_f = 36$, and $g_g = 16$, $s_{\text{SB}}/T^3 \simeq 34.62$ while $(\rho - 3p)/T^4 \rightarrow 0$. Therefore, at high temperatures, ζ/s tends to very small values.

In light of this, the physical meaning of the ζ/s reflects with it the impacts of the entropy. Thus, ζ/s could be interpreted as bulk viscosity per degree of freedom. The latter varies from phase (hadron) to phase (QGP). In the section that follows, we focus of ζ at varying energy density.

B. Bulk viscosity in non-perturbative and perturbative calculations

1. QCD contributions

The relaxation time $\tau_f(T)$ plays an essential role in estimating ζ . As introduced in section II A 1, $\tau_f(T)$ involves complicated collision integrals. Using cross section and mean collision time, i.e. thermal averages [23, 24, 28] led to Eq. (6). Fig. 4 depicts the temperature dependence of τ as calculated in non-perturbative and perturbative QCD simulations [9–12] to which contributions from quark and gluon condensates, section II B and II C, respectively, and thermodynamics from gauge bosons, charged leptons, and Higgs bosons are added. We notice that τ steadily decreases with increasing T . In the different phases, there are different rates of τ -decrease.

Left panel of Fig. 5 shows the temperature dependence of $9\omega_0\zeta/Ts$. Here, we cover temperatures ranging from 100 MeV up to 1 TeV. The bulk viscosity is calculated according to Eq. (68), in which the thermodynamic quantities, s/T^3 , c_s^2 and $(\rho - 3p)/T^4$ are taken from non-perturbative [9] and perturbative QCD calculations [10, 11]. As elaborated in ref. [12], both sets of calculations are properly rescaled. It was assumed that the non-perturbative effects [9] characterize the resulting thermodynamics at temperatures ≤ 10 GeV, especially

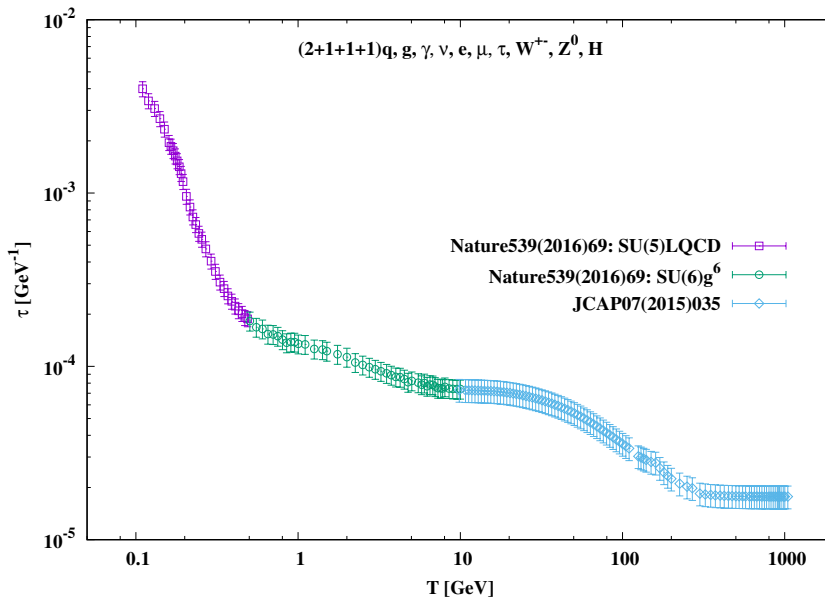


Fig. 4: (Color online) The temperature dependence of τ as calculated at vanishing baryon-chemical potential as estimated from non-perturbative and perturbative QCD simulations, from quark and gluon condensates and from thermodynamics of gauge bosons, charged leptons, and Higgs bosons.

that the heavier quarks have been also included. At higher temperatures, the thermodynamic quantities such as pressure, energy density, and entropy density can also be calculated, perturbatively. The results reported in refs. [10, 11] cover temperatures up to 1 TeV. With a scaling proposed in ref. [12], both calculations become matching with each others, perfectly smoothly. These allow the temperatures to go over the TeV-scale. It was found that the analysis using the lattice simulations [9–11] consistently characterizes QCD and EW domains. Accordingly, both have crossover transitions. From the phenomenological point of view, it was highlighted that the QCD phase transition seems stronger than the thermal EW phase transition. With the regard of possible implications, the temperature dependence of $9\omega_0\zeta/Ts$ can be applied on heavy-ion collisions [90], for instance.

The reason that we start with $9\omega_0\zeta/Ts$ vs. T in GeV units, is an intention to compare with refs. [6, 89]. Indeed, above T_c , $9\omega_0\zeta/Ts$ rapidly declines. In the present script, we go beyond the limit of $3 - 4 T_c$ as done in ref. [6]. We use $2 + 1 + 1 + 1$ lattice QCD and add our estimation for the temperature dependence of up, down, strange, and charm quark condensates from PLSM, Fig. 2, together with the gluon condensates, Eqs. (50)-(54). The temperature dependence of the quark and gluon condensates are depicted as solid curves in left panel of Fig. 5, whose y-axis is positioned to the right. Despite the limitation up to the charm quark, it is obvious that the contributions from the quark and gluon condensates are responsible for the relative large $9\omega_0\zeta/Ts$ comparing to the results reported in ref. [6]. Up to ~ 2 GeV, the temperature dependence of the four quark condensates vanishes. At temperatures larger than ~ 2 GeV, condensates of heavier quarks likely become dominant. Also, in this limit, the temperature dependence of the gluon condensates vanishes, as the interaction measure becomes very small, Eq. (51), at least within the QCD sector.

Similar to the peak at the QCD crossover, there is a signature for EW crossover at about 60 GeV. As pointed out in Fig. 1 of ref. [12], the EW crossover, as the name says, seems to take place within a wide range of temperatures, from ~ 20 to ~ 100 GeV. That $9\omega_0\zeta/Ts$ is conjectured to play the role of an order parameter is comprehend, as it strongly depends on the thermodynamic quantities, entropy, speed of sound squared, and interaction measure besides the quark and gluon condensates. Each of them reflects rapid change when going through phase transition. The reason why $9\omega_0\zeta/Ts$ nearly vanishes below ~ 20 and above ~ 100 GeV would be the absence of bottom and top quark condensates. They likely heighten the values of $9\omega_0\zeta/Ts$ including the peak at about 60 GeV, as well.

The bottom panel shows the bulk viscosity ζ as a function of the energy density ρ . Both quantities are given in physical units. Such a barotropic dependence can be straightforwardly applied in various cosmological

aspects [21, 23–25] in the way that ρ can be directly substituted by H , the Hubble parameter. We compare between QCD (bottom curve) and SM contributions (top curve). The earlier counts for the thermodynamic quantities calculated in lattice QCD [9–12]. The latter takes into account contributions from quark and gluon condensates and thermodynamics of an ideal gas of gamma, charged leptons, W^\pm , Z^0 and H bosons.

We notice that different than the temperature dependence (left panel), here the dependence of QCD ζ on ρ is very structured, i.e. a non-monotonic dependence. At least, there are four domains to be distinguished. The first one is the hadron-QGP phase (Hadron-QGP). This region spans over $\rho \lesssim 100 \text{ GeV/fm}^3$. In the second phase, ζ reaches another maximum. Here, ρ covers up to $\sim 5 \times 10^7 \text{ GeV/fm}^3$. Accordingly, it would be assumed that this domain combines QCD and EW eras (QCD). The third phase seems to form an asymmetric parabola (EW), where the focus is likely positioned at the corresponding critical energy density, $\rho_c \simeq 10^{12} \text{ GeV/fm}^3$. The fourth region shows a rapid increase in ρ emerging from non-continuous point. It seems very likely that asymmetric parabola can be constructed in each region.

First, Hadron-QGP is characterized by a rapid increase in ζ , i.e. $\zeta \simeq 1 \text{ GeV}^3$, at $\rho \simeq 1 \text{ GeV/fm}^3$. This is then followed by a slight increase in ζ . For example, at $\rho \simeq 100 \text{ GeV/fm}^3$, ζ becomes to $\sim 130 \text{ GeV}^3$. One could estimate that the hadron phase would be defined by $\rho \lesssim 0.5 \text{ GeV/fm}^3$ [92, 93], at which $\zeta \lesssim 0.5 \text{ GeV}^3$. On the other hand, QGP is accommodated, at $0.5 \lesssim \rho \lesssim 100 \text{ GeV/fm}^3$, i.e. much wider ρ than the hadron phase. An essential conclusion could be drawn now. Over this wide range of ρ , the bulk viscosity is obviously not only finite but large, which could be aligned with the RHIC discovery of strongly correlated QGP [1–3].

At higher energy densities, there is a tendency of an increase in ζ with increasing ρ . A peak is nearly positioned at $\rho \simeq 5 \times 10^6 \text{ GeV/fm}^3$ and $\zeta \simeq 200 \text{ GeV}^3$. This would refer to a smooth transition from QCD to EW matter. Precise estimation for the critical quantities and suitable order parameters shall be subject of a future study. To summarize, we recall that over a region, where ρ gets an huge increase of about five-order-of-magnitude; $10^2 \lesssim \rho \lesssim 5 \times 10^7 \text{ GeV/fm}^3$, there a small increase followed by a small decrease in ζ to be quantified.

The huge jump in ζ takes place when ρ increases from nearly 10^8 to approximately 10^{12} GeV/fm^3 . The corresponding bulk viscosity increases from nearly 3×10^2 to approximately $5 \times 10^9 \text{ GeV}^3$. A further increase in ρ of about one-order-of-magnitude seems not affecting ζ . But with the continuation of the increasing of ρ of about two-order-of-magnitude, we notice that ζ declines to $\sim 3 \times 10^5 \text{ GeV/fm}^3$.

2. SM contributions

Besides gluons and $(2 + 1 + 1 + 1)$ quarks, the contributions of the gauge bosons: photons, W^\pm , and Z^0 , the charged leptons: neutrino, electron, muon, and tau, and the Higgs bosons: scalar Higgs particle, are also taken into account [12]. Obviously, as much as possible SM contributions are included in the present calculations. The vacuum and thermal bottom quark condensate, the entire gravitational sector, neutral leptons, and top quark are the missing SM-contributions. The results are shown in Fig. 5, as well. An overall conclusion can be drawn now. The SM contributions are very significant over the entire ranges of temperatures and energy densities. On one hand, they allow to cover higher temperatures and larger energy densities. On the other hand, the characteristic structures observed with the QCD contributions, section sec:QCDconts, is almost removed, so that the dependence on temperature (left panel) and on energy density (right panel) becomes almost monotonic. Last but not least, the temperature dependence of $9\omega_0\zeta/Ts$ is exponentially decreasing, while the energy-density dependence of ζ is almost linearly increasing.

For $9\omega_0\zeta/Ts$, the resulting parameterizations are

$$\text{Hadron - QGP : } \frac{9\omega_0\zeta}{Ts} = a_1 + a_2 \exp[-a_3 (T^{a_4})], \quad (70)$$

$$\text{QCD : } \frac{9\omega_0\zeta}{Ts} = b_1 + b_2 \exp[-b_3 (T^{b_4})], \quad (71)$$

$$\text{EW : } \frac{9\omega_0\zeta}{Ts} = c_1 + c_2 T + c_3 \exp[-c_4 (T^{c_5})]. \quad (72)$$

For Hadron-QGP: $a_1 = 1.624 \pm 0.054 \text{ GeV}$, $a_2 = 29.004 \pm 2.94 \text{ GeV}$, $a_3 = 22.776 \pm 2.829$, and $a_4 = 1.451 \pm 0.101$. For QCD: $b_1 = 0.7629 \pm 0.081 \text{ GeV}$, $b_2 = 4.811 \pm 1.613 \text{ GeV}$, $b_3 = 2.291 \pm 1.432$, and $b_4 = 0.226 \pm 0.174$. For EW: $c_1 = 0.404 \pm 0.003 \text{ GeV}$, $c_2 = -5.827 \times 10^{-6} \pm 1.611 \times 10^{-6}$, $c_3 = 0.490 \pm 0.005 \text{ GeV}$, $c_4 = 0.0036 \pm 0.0003$, and $c_5 = 1.218 \pm 0.021$. There is a rapid decrease in $9\omega_0\zeta/Ts$ at temperatures characterizing the hadronic matter,

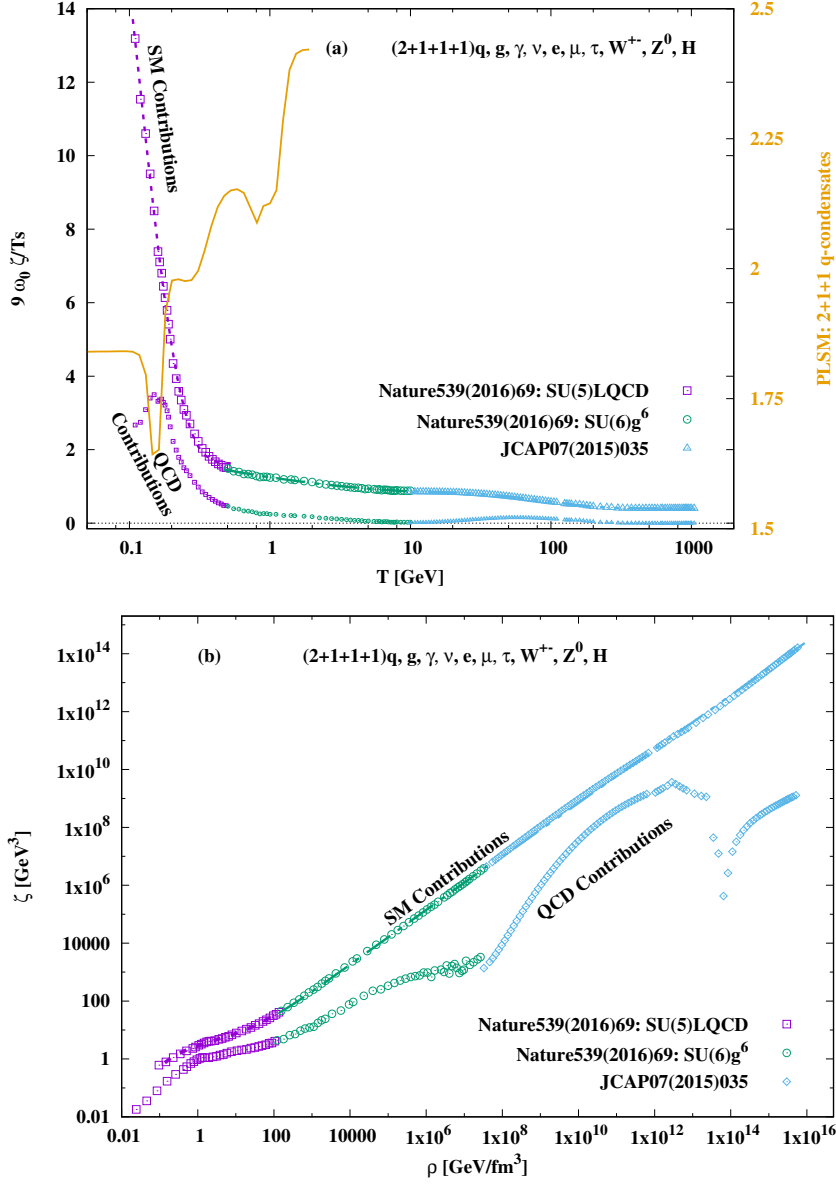


Fig. 5: (Color online) Top panel depicts the dimensionless $9\omega_0\zeta/Ts$ vs. T in GeV units. Bottom panel shows the bulk viscosity ζ in dependence of the energy density ρ . Both quantities are calculated at vanishing baryon-chemical potential and given in physical units. The top symbols stand for the SM contributions, section III B 2, while the bottom ones stand for the QCD contributions. The solid curve (left panel) represent the vacuum and thermal gluon and quark (u , d , s , and c) condensates, sections II B, II C, and Fig. 2. The dashed curves in the bottom panel represent parameterizations, section III B 2.

Eq. (70). With a slower rate, this seems to continue within the QGP, at temperatures up to *sim*10 GeV, Eq. (71). At $T > 10$ GeV, the decrease combines linear and exponential functions, Eq. (72).

For $\zeta(\rho)$, we distinguish three regions with the parameterizations

$$\text{Hadron} - \text{QGP} : \quad \zeta = d_1 + d_2\rho + d_3\rho^{d_4}, \quad (73)$$

$$\text{QCD} : \quad \zeta = e_1 + e_2\rho^{e_3}, \quad (74)$$

$$\text{EW} : \quad \zeta = f_1 + f_2\rho^{f_3}. \quad (75)$$

For Hadron-QCD: $d_1 = -9.336 \pm 4.152$, $d_2 = 0.232 \pm 0.003$, $d_3 = 11.962 \pm 4.172$, and $d_4 = 0.087 \pm 0.029$. For QCD: $e_1 = 8.042 \pm 0.056$, $e_2 = 0.301 \pm 0.002$, and $e_3 = 0.945 \pm 0.0001$. For EW: $f_1 = 0.350 \pm 0.065$, $f_2 = 10.019 \pm 0.934$, and $f_3 = 0.929 \pm 8.898 \times 10^{-5}$.

IV. CONCLUSIONS

Comparing our HRGM- and PLSM-results of bulk viscosity with the first-principle QCD calculations, we concluded a convincing agreement at temperatures exceeding the QCD scale and an excellent integrability below this range of temperatures. Hence, the methodology utilized in the present work, namely BUU and KG approaches, could be confirmed.

Allowing temperatures to increase from a few MeV up to TeV and energy densities up to 10^{16} GeV/fm³, almost all possible contributions to the bulk viscosity are taken into consideration. The first type of contributions represents thermodynamic quantities calculated in non-perturbation and perturbation QCD with up, down, strange, charm, and bottom quark flavors and, of course, the entire gluonic sector. Taking into account contributions of the gauge bosons: photons, W^\pm , and Z^0 , the charged leptons: neutrino, electron, muon, and tau, and the Higgs bosons: scalar Higgs particle, shows that these Standard Model particles are very significant, especially when bearing in mind cosmological implications, for instance. When comparing the results of bulk viscosity with and without this sector, we conclude that both temperature and energy-density dependences become to a great extent monotonic. Furthermore, this sector considerably adds to the results so that the energy density approaches about two-order-of-magnitude GeV/fm³ larger than the perturbation theory. The vacuum and thermal condensations of gluons and quarks (up, down, strange, and charm) as calculated in the Polyakov linear-sigma model are the third type of contributions.

We conclude that the bulk viscosity increases almost linearly with increasing energy density. Opposite to such a dependence is the one of the dimensionless quantity $9\omega_0\zeta/Ts$ on temperature, where ω_0 is a perturbative scale and s is the entropy density. Here, an almost linearly decrease with increasing temperature was obtained.

Acknowledgements

The work of AT was supported by the ExtreMe Matter Institute (EMMI) at the GSI Helmholtz Centre for Heavy Ion Research.

-
- [1] M. Gyulassy and L. McLerran, Nucl. Phys. **A750**, 30 (2005).
 - [2] U. Heinz, C. Shen, and H. Song, AIP Conf. Proc. **1441**, 766 (2012).
 - [3] S. Ryu et al., Phys. Rev. **C97**, 034910 (2018).
 - [4] P. Kovtun, D. T. Son, and A. O. Starinets, Phys. Rev. Lett. **94**, 111601 (2005).
 - [5] S. Sakai and A. Nakamura, PoS **LATTICE2007**, 221 (2007).
 - [6] F. Karsch, D. Kharzeev, and K. Tuchin, Phys. Lett. **B663**, 217 (2008).
 - [7] D. Roder, J. Ruppert, and D. H. Rischke, Phys. Rev. **D68**, 016003 (2003).
 - [8] A. M. Abdel Aal Diab and A. N. Tawfik, EPJ Web Conf. **177**, 09005 (2018).
 - [9] S. Borsanyi et al., Nature **539**, 69 (2016).
 - [10] M. Laine and M. Meyer, JCAP **1507**, 035 (2015).
 - [11] M. D’Onofrio and K. Rummukainen, Phys. Rev. **D93**, 025003 (2016).
 - [12] A. N. Tawfik and I. Mishustin, (2019).
 - [13] Z. Hu, N. T. Leonardo, T. Liu, and M. Haytmyradov, Int. J. Mod. Phys. **A32**, 1730015 (2017).
 - [14] N. Aghanim et al., (2018).
 - [15] L. Adamczyk et al., Phys. Rev. **C98**, 014915 (2018).
 - [16] P. Boek, Phys. Rev. **C95**, 054909 (2017).
 - [17] L. Adamczyk et al., Phys. Rev. **C96**, 044904 (2017).
 - [18] A. Tawfik and M. Wahba, Annalen Phys. **522**, 849 (2010).
 - [19] P. Chakraborty and J. I. Kapusta, Phys. Rev. **C83**, 014906 (2011).
 - [20] B. Cheng, Phys. Lett. **A160**, 329 (1991).

- [21] A. Tawfik, T. Harko, H. Mansour, and M. Wahba, *Uzbek J. Phys.* **12**, 316 (2010).
- [22] C. P. Singh, *Pramana* **71**, 33 (2008).
- [23] A. Tawfik and T. Harko, *Phys. Rev.* **D85**, 084032 (2012).
- [24] A. Tawfik, M. Wahba, H. Mansour, and T. Harko, *Annalen Phys.* **523**, 194 (2011).
- [25] A. Tawfik, M. Wahba, H. Mansour, and T. Harko, *Annalen Phys.* **522**, 912 (2010).
- [26] S. Weinberg, *The Quantum theory of fields. Vol. 1: Foundations*, Cambridge University Press, 2005.
- [27] A. N. Tawfik, A. M. Diab, and T. M. Hussein, *Int. J. Adv. Res. Phys. Sci.* **3**, 4 (2016).
- [28] A. N. Tawfik, A. M. Diab, and M. T. Hussein, *Int. J. Mod. Phys.* **A31**, 1650175 (2016).
- [29] R. Marty, E. Bratkovskaya, W. Cassing, J. Aichelin, and H. Berrehrach, *Phys. Rev.* **C88**, 045204 (2013).
- [30] R. Kubo, *J. Phys. Soc. Jap.* **12**, 570 (1957).
- [31] D. N. Zubarev and P. Shepherd, *Nonequilibrium statistical thermodynamics*, Consultants Bureau New York, 1974.
- [32] S. Ghosh, *Int. J. Mod. Phys.* **A29**, 1450054 (2014).
- [33] R. Lang, N. Kaiser, and W. Weise, *Eur. Phys. J.* **A48**, 109 (2012).
- [34] D. Fernandez-Fraile and A. Gomez Nicola, *Eur. Phys. J.* **C62**, 37 (2009).
- [35] A. Grozin, Lectures on QED and QCD, in *3rd Dubna International Advanced School of Theoretical Physics Dubna, Russia, January 29-February 6, 2005*, pages 1–156, 2005.
- [36] S. J. Brodsky and R. Shrock, *Proc. Nat. Acad. Sci.* **108**, 45 (2011).
- [37] M. Gell-Mann, R. J. Oakes, and B. Renner, *Phys. Rev.* **175**, 2195 (1968).
- [38] M. Schumacher, *Pramana* **87**, 44 (2016).
- [39] B. L. Ioffe, *Phys. Atom. Nucl.* **66**, 30 (2003), [*Yad. Fiz.*66,32(2003)].
- [40] S. Weinberg, *Phys. Rev. Lett.* **17**, 616 (1966).
- [41] A. Tawfik and D. Toublan, *Phys. Lett.* **B623**, 48 (2005).
- [42] M. Tanabashi et al., *Phys. Rev.* **D98**, 030001 (2018).
- [43] S. Aoki et al., *Eur. Phys. J.* **C77**, 112 (2017).
- [44] H. Leutwyler, *Scholarpedia* **7**, 8708 (2012), revision #138476.
- [45] M. Gell-Mann, *Phys. Rev.* **125**, 1067 (1962).
- [46] C. McNeile et al., *Phys. Rev.* **D87**, 034503 (2013).
- [47] C. T. H. Davies et al., *Phys. Rev.* **D100**, 034506 (2019).
- [48] J. Gasser and H. Leutwyler, *Phys. Lett.* **B184**, 83 (1987).
- [49] J. T. Lenaghan, D. H. Rischke, and J. Schaffner-Bielich, *Phys. Rev.* **D62**, 085008 (2000).
- [50] M. A. Shifman, A. I. Vainshtein, and V. I. Zakharov, *Nucl. Phys.* **B147**, 448 (1979).
- [51] A. Deur, S. J. Brodsky, and G. F. de Teramond, *Prog. Part. Nucl. Phys.* **90**, 1 (2016).
- [52] D. E. Miller and A.-N. M. Tawfik, *Acta Phys. Polon.* **B35**, 2165 (2004).
- [53] D. E. Miller and A.-N. M. Tawfik, *J. Phys.* **G30**, 731 (2004).
- [54] D. E. Miller and A.-N. M. Tawfik, *Appl. Math. Inf. Sci.* **5**, 239 (2011).
- [55] D. E. Miller and A. N. Tawfik, *Indian J. Phys.* **86**, 1021 (2012).
- [56] D. E. Miller and A.-N. Tawfik, *Fizika* **B16**, 17 (2007).
- [57] P. Colangelo, F. Giannuzzi, S. Nicotri, and F. Zuo, *Phys. Rev.* **D88**, 115011 (2013).
- [58] M. Gell-Mann and M. Levy, *Nuovo Cim.* **16**, 705 (1960).
- [59] J. S. Schwinger, *Annals Phys.* **2**, 407 (1957).
- [60] J. S. Schwinger, *Phys. Rev.* **82**, 914 (1951).
- [61] J. S. Schwinger, *Phys. Rev.* **91**, 713 (1953).
- [62] J. Schwinger, *Phys. Rev.* **91**, 728 (1953).
- [63] J. Schwinger, *Phys. Rev.* **92**, 1283 (1953).
- [64] J. Schwinger, *Phys. Rev.* **93**, 615 (1954).
- [65] J. Schwinger, *Phys. Rev.* **94**, 1362 (1954).
- [66] S. Gasiorowicz and D. A. Geffen, *Rev. Mod. Phys.* **41**, 531 (1969).
- [67] M. C. Birse, *J. Phys.* **G20**, 1537 (1994).
- [68] S. Gallas, F. Giacosa, and D. H. Rischke, *Phys. Rev.* **D82**, 014004 (2010).
- [69] A. N. Tawfik and A. M. Diab, *Phys. Rev.* **C91**, 015204 (2015).
- [70] C. Wesp, H. van Hees, A. Meistrenko, and C. Greiner, *Eur. Phys. J.* **A54**, 24 (2018).
- [71] A. N. Tawfik, A. M. Diab, and M. T. Hussein, *J. Phys.* **G45**, 055008 (2018).
- [72] A. N. Tawfik, A. M. Diab, and M. T. Hussein, *Chin. Phys.* **C43**, 034103 (2019).
- [73] A. N. Tawfik, C. Greiner, A. M. Diab, M. T. Ghoneim, and H. Anwer, (2019).
- [74] A. N. Tawfik, A. M. Diab, N. Ezzelarab, and A. G. Shalaby, *Adv. High Energy Phys.* **2016**, 1381479 (2016).
- [75] A. N. Tawfik, A. M. Diab, and M. T. Hussein, *J. Exp. Theor. Phys.* **126**, 620 (2018).
- [76] A. N. Tawfik, A. M. Diab, M. T. Ghoneim, and H. Anwer, (2019).
- [77] A. Tawfik, N. Magdy, and A. Diab, *Phys. Rev.* **C89**, 055210 (2014).
- [78] A. N. Tawfik and N. Magdy, *Phys. Rev.* **C90**, 015204 (2014).

- [79] C. Ratti, M. A. Thaler, and W. Weise, Phys. Rev. **D73**, 014019 (2006).
- [80] B.-J. Schaefer, J. M. Pawłowski, and J. Wambach, Phys. Rev. **D76**, 074023 (2007).
- [81] S. Roessner, C. Ratti, and W. Weise, Phys. Rev. **D75**, 034007 (2007).
- [82] K. Fukushima, Phys. Rev. **D77**, 114028 (2008), [Erratum: Phys. Rev.D78,039902(2008)].
- [83] P. M. Lo, B. Friman, O. Kaczmarek, K. Redlich, and C. Sasaki, Phys. Rev. **D88**, 074502 (2013).
- [84] J. I. Kapusta and C. Gale, *Finite-temperature field theory: Principles and applications*, Cambridge Monographs on Mathematical Physics, Cambridge University Press, 2011.
- [85] A. M. Polyakov, Phys. Lett. **72B**, 477 (1978).
- [86] L. Susskind, Phys. Rev. **D20**, 2610 (1979).
- [87] K. Fukushima, Phys. Lett. **B591**, 277 (2004).
- [88] D. Kharzeev and K. Tuchin, JHEP **09**, 093 (2008).
- [89] J. Noronha-Hostler, J. Noronha, and C. Greiner, Phys. Rev. Lett. **103**, 172302 (2009).
- [90] J. E. Bernhard, J. S. Moreland, S. A. Bass, J. Liu, and U. Heinz, Phys. Rev. **C94**, 024907 (2016).
- [91] J. Letessier and J. Rafelski, *Hadrons and quark - gluon plasma*, volume 18, Cambridge University Press, 2002.
- [92] A. Tawfik, Phys. Rev. **D71**, 054502 (2005).
- [93] A. Tawfik, J. Phys. **G31**, S1105 (2005).